Journal of Applied Polymer Science

A novel approach for extracting cellulose nanofibers from lignocellulosic biomass by ball milling combined with chemical treatment

Md. Nuruddin, Mahesh Hosur, Md. Jamal Uddin, David Baah, Shaik Jeelani
Department of Materials Science and Engineering, Tuskegee University, Tuskegee, Alabama 36088
Correspondence to: M. Hosur (E-mail: hosur@mytu.tuskegee.edu)

ABSTRACT: Cellulose nanofibers (CNFs) were isolated from kenaf fibers and wheat straw by formic acid (FA)/acetic acid (AA), peroxyformic acid (PFA)/peroxyacetic acid (PAA), hydrogen peroxide (H_2O_2) treatment; and subsequently through ball milling treatment. Characterization of extracted cellulose and cellulose nanofibers was carried out through Fourier transform infrared spectroscopy (FTIR), scanning electron microscopy (SEM), transmission electron microscopy (TEM), X-ray diffraction (XRD), and thermogravimetric analysis (TGA). TEM images showed that extracted cellulose nanofibers had diameter in the range of 8–100 nm. FTIR and XRD results implied that hemicellulose and lignin were mostly removed from lignocellulosic biomass with an increase in crystallinity, and isolation of cellulose nanofibers was successful. The TGA results showed that decomposition temperature of cellulose nanofibers increased by about 27°C when compared with that of untreated lignocellulosic biomass. No significant change was observed in the decomposition temperature of bleached celluloses after ball milling. © 2015 Wiley Periodicals, Inc. J. Appl. Polym. Sci. **2016**, *133*, 42990.

KEYWORDS: biodegradable; cellulose and other wood products; X-ray

Received 15 July 2015; accepted 28 September 2015
DOI: 10.1002/app.42990

INTRODUCTION

Lignocellulosic biomass, the world's most abundant renewable resource has been considered as a valuable natural raw material for pulp and paper industry and high performance biocomposites.[1–3] In addition to this, some useful chemical compounds such as ethanol and lignin modified phenol-formaldehyde resin can be produced.[4–8]

Cell wall of lignocellulosic biomass comprises of lignin, hemicellulose, cellulose, small quantity of pectin, and extractives. Cellulose is the world's most abundant biopolymer, which consists of linear homopolysaccharide composed of unbranched β-(1,4)-D-glucose units linked together by β-1-4-linkages. Each monomer glucose unit carries three hydroxyl groups. Three hydroxyl groups shown in the Figure 1, located at the position of C2 and C3 (secondary hydroxyl groups) and C6 (primary hydroxyl groups) can form intra and inter molecular hydrogen bonds which provide highly ordered three-dimensional crystalline structure. Thus, these hydroxyl groups being able to form hydrogen bonds control the physical properties of cellulose.[9]

Cellulose nanofibers (CNFs) have gained significant attention due to their wide range of applications such as nanocomposites,[10] regenerative medicine,[11] automotive[12] because of their high aspect ratio (L/d), easily availability, biocompatibility, and renewability,[13] excellent mechanical properties (high specific strength and modulus),[14] large specific surface area, low coefficient of thermal expansion, environmental benefits, and low cost.[15]

Several methods have been utilized for isolation of cellulose nanoparticles (cellulose nanofibers, cellulose microfibrils, and cellulose nanowhiskers) from lignocelluloses. These methods include acid hydrolysis treatment[3,16–18]; high-pressure homogenizer[19,20]; enzyme assisted hydrolysis[21,22]; 2,2,6,6-tetramethylpiperidin-1-yloxy (TEMPO) catalyzed oxidation[23,24]; and ultrasonication technique.[25–27] All of these methods isolate cellulose nanofibers depending upon type of raw material and also the pretreatment process.

Ball milling is an environmental-friendly and low cost method, which uses friction, collision, shear or other mechanical actions to modify the crystalline structure of materials, such as alloys[28] and polymers.[29] It also has been used to change structure of cellulose either in dry or solvent-assisted wet condition. Ball milling in dry condition has been used to increase the amorphous content of celluloses,[30,31] while wet ball milling technique utilizes different solvents to transform cellulose I to cellulose II and noncrystalline cellulose.[32,33] Celluloses have crystalline regions due to strong hydrogen bonding[34] and Van der Waals

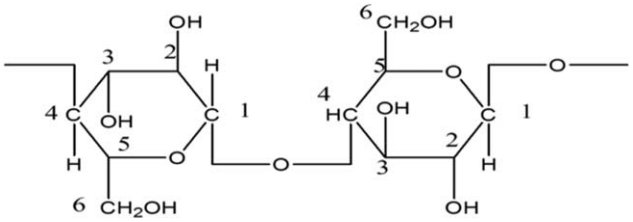

Figure 1. Schematic diagram of cellulose.

forces[35] between the cellulose molecules. This strong bonding makes them more resistance toward chemicals and enzymes attack. Therefore, it is very important to break down this hydrogen bonding to facilitate conversion of cellulose to biofuel.[36] Ball milling technique has been employed to convert crystalline cellulose to amorphous cellulose in order to facilitate the production of biofuel.[36,37] Although, numerous studies are reported in literature about conversion of cellulose into amorphous cellulose and cellulose II, to the best of our knowledge, no study has been reported on the effect of ball milling for isolation of cellulose nanofibers.

In the current work, cellulose nanofibers were extracted from kenaf fibers and wheat straw via formic acid (FA)/acetic acid (AA), peroxyformic acid (PFA)/peroxyacetic acid (PAA), and hydrogen peroxide (H_2O_2) treatment followed by ball milling at different time intervals. Morphology, crystallinity, and thermal stability of raw biomass, bleached cellulose, and ball milled cellulose nanofibers (CNFs) were investigated and compared to determine the effect of ball milling on celluloses.

EXPERIMENTAL

Materials

Natural biomasses (wheat straw and kenaf fibers) were collected from Home Depot, Georgia. Various chemicals used for extraction of cellulose and cellulose nanofibers (CNFs) such as Formic acid, Acetic acid, Ethanol, Hydrogen peroxide, Sodium hydroxide, and other chemicals were purchased from Sigma-Aldrich.

Extraction of Celluloses

Cellulose was extracted from wheat straw and kenaf fibers according to Watkins *et al.*[38] Biomass was cut into small sizes, taken in a conical flask and mixed with 85% organic acid solution (the ratio of formic acid to acetic acid was 70:30 by volume and acid solution to fiber ratio was 8:1). The mixture was refluxed on a hot plate at 110°C for 2 h. After completion of reaction time, the fibers were filtered in a Buchner funnel and washed with 80% formic acid followed by hot distilled water. This process partially removes hemicellulose and lignin. After this process, organic acid treated biomass was further treated with peroxyformic acid (PFA)/peroxyacetic acid (PAA) in hot water bath at 80°C for 2 h to remove additional hemicellulose and lignin. The mixture of PFA/PAA was prepared by adding 8 mL of 35% H_2O_2 with 85% formic acid/acetic acid mixture (fiber to organic acid ratio was 1:5 by w/v basis). Finally, the residue was filtered to separate cooking liquor (lignin and hemicelluloses mixed with organic acid) from cellulose and washed with hot water. However, this treatment does not ensure complete removal of hemicellulose and lignin. In order to additional removal of lignin and hemicellulose, bleaching treatment is required. In this study, bleaching was carried out with 35% H_2O_2 solution (hydrogen peroxide to fiber ratio 4%) and NaOH solution (to maintain pH: 11–12), in a hot water bath at 80°C for 2 h. Finally, the pulp was washed several times with distilled water to ensure significant removal of residual lignin and hemicellulose.

Preparation of Cellulose Nanofibers (CNFs)

Approximately 10 g of cellulose obtained after bleaching was mixed with 10 mL of 80% ethanol and the mixture was subjected to ball milling for different time intervals (30, 60, 90, and 120 min) in a Mixer/Mill 8000D^{TM} (SPEX Sample Prep) using zirconia ceramic grinding vial and 12.7 mm diameter balls. After ball milling, the mixture was repeatedly washed with distilled water and centrifuged until the pH of the cellulose reaches between 6 and 7. A schematic of breaking down of cellulose into cellulose nanofibers is shown in Figure 2.

Scanning Electron Microscopy (SEM)

Morphological studies were conducted on as received kenaf fiber, wheat straw, bleached cellulose, and ball milled CNFs using JEOL JSM-6400 scanning electron microscope (SEM) using 20 kV accelerating voltage. Surface of each sample was sputtered with thin layer of gold before SEM was conducted. The diameter of bleached cellulose from SEM images was determined by using Image J software. At least 50 measurements were taken to plot the size distribution curve of bleached celluloses.

Transmission Electron Microscopy (TEM)

A drop of dilute cellulose nanofibers (CNFs) suspension was deposited on the 300 mesh Formvar/Carbon coated support film grids. Excess liquid was removed through absorption using a piece of filter paper and allowed to dry at room temperature. The dried sample was observed under ZEISS EM10 Transmission Electron Microscope (Thornwood, NY) operated at 60 KV accelerating voltage. The diameter of the cellulose nanofibers (CNFs) was calculated from TEM images using MaxIm DL5

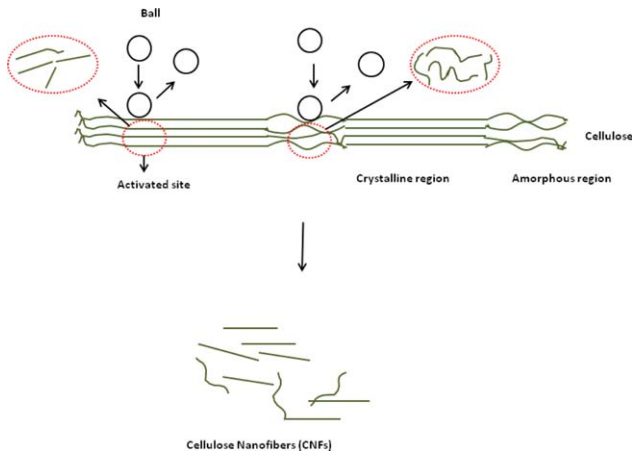

Figure 2. Schematic diagram of ball milling of cellulose. [Color figure can be viewed in the online issue, which is available at wileyonlinelibrary.com.]

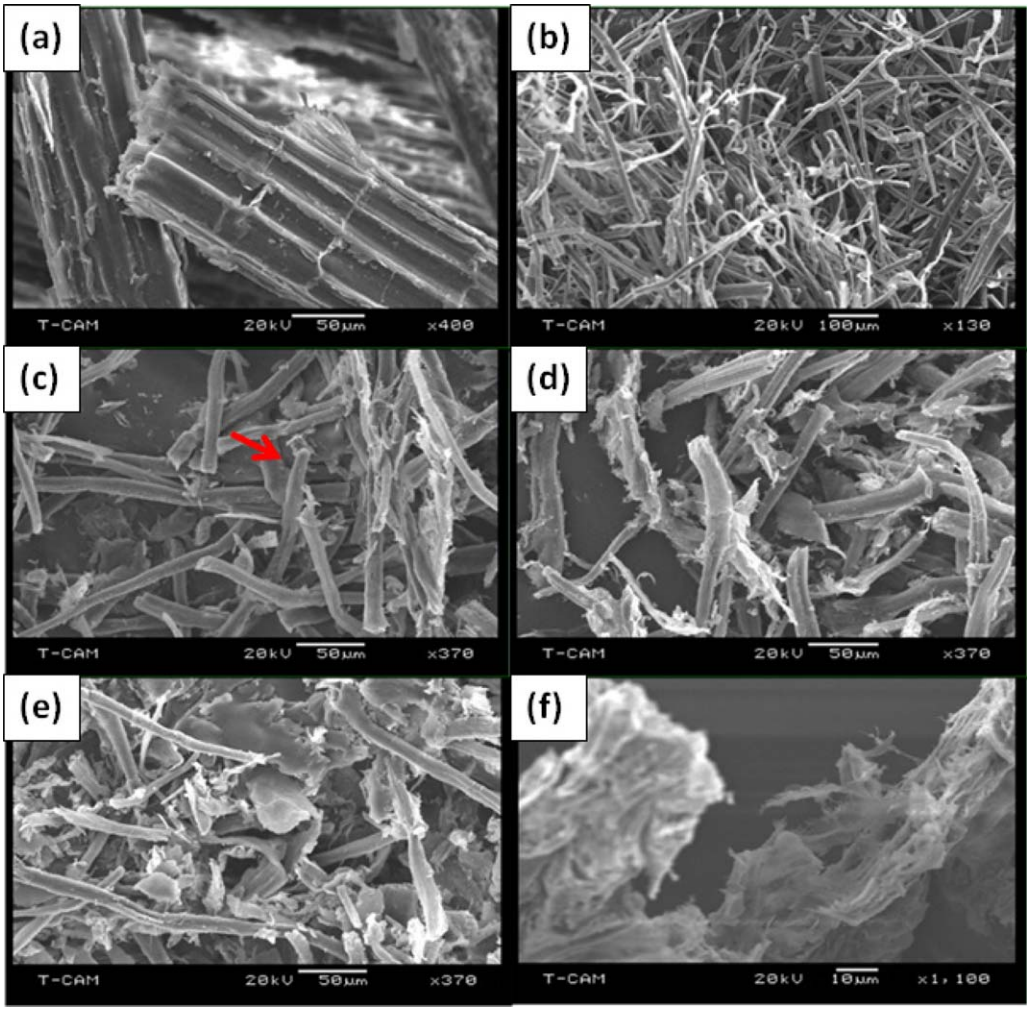

Figure 3. SEM micrograph of (a) kenaf fiber, (b) cellulose, (c) B-30 mins, (d) B-60 mins, (e) B-90 mins, and (f) B-120 mins (CNFs). [Color figure can be viewed in the online issue, which is available at wileyonlinelibrary.com.]

software. At least 50 measurements were taken to plot the size distribution curve of cellulose nanofibers.

Fourier Transform-Infrared (FTIR) Spectroscopy

Structural characterization was conducted on samples stated above using FTIR. Shimadzu FTIR 8400s equipped with MIRacle^{TM} attenuated total reflection (ATR) was used and scans were acquired in between 650–3500 cm^{-1} with a resolution of 4 cm^{-1}.

X-ray Diffraction (XRD)

The X-ray diffraction (XRD) patterns were measured for kenaf fibers, wheat straw, bleached cellulose, and isolated cellulose nanofibers with Rigaku X-ray diffractometer using Cu Kα radiation at 40 kV and 30 mA. Scattered radiation was detected in the range of $2\theta = 5$–40° at a scan rate of 5°/min. The crystallinity index (CI) was calculated from the heights of the 200 peak (I_{200}, $2\theta = 22.4^\circ$) and the intensity minimum between the 200 and 110 peaks (I_{am}, $2\theta = 18.32^\circ$) using the Segal method which gives crystallinity index as $(I_{200}–I_{am})/I_{200}$ times 100, where I_{200} and I_{am} represent crystalline and amorphous peaks, respectively.

Thermo gravimetric analysis (TGA)

Thermal stabilities of untreated kenaf fibers, wheat straw, bleached cellulose, and CNFs were characterized using Q500 system from TA Instruments (Delaware). Sample weight for test was maintained at about 10 mg. TGA scans were performed under nitrogen environment with a purge flow rate of 60 mL/min and heating from 25 to 600°C at 10°C/min rate.

RESULTS AND DISCUSSION

Morphological and Structural Characterization

SEM images of untreated wheat straw, kenaf fiber, bleached cellulose, ball milled celluloses, and extracted nanocelluloses are shown in Figures 3 and 4. Natural fiber is a composite material in which cellulose acts as the main reinforcement. Other components like lignin and pectin act as binding materials. In the current study, we observed from SEM images that untreated wheat straw and kenaf fiber display lot of non-cellulosic components (lignin and pectin) scattered over the fiber (cellulosic part) surface, acting as cementing materials which bind several cellulosic microfibrils together. Similar observation was reported by Penjumras *et al.*[39] The diameter of untreated wheat straw

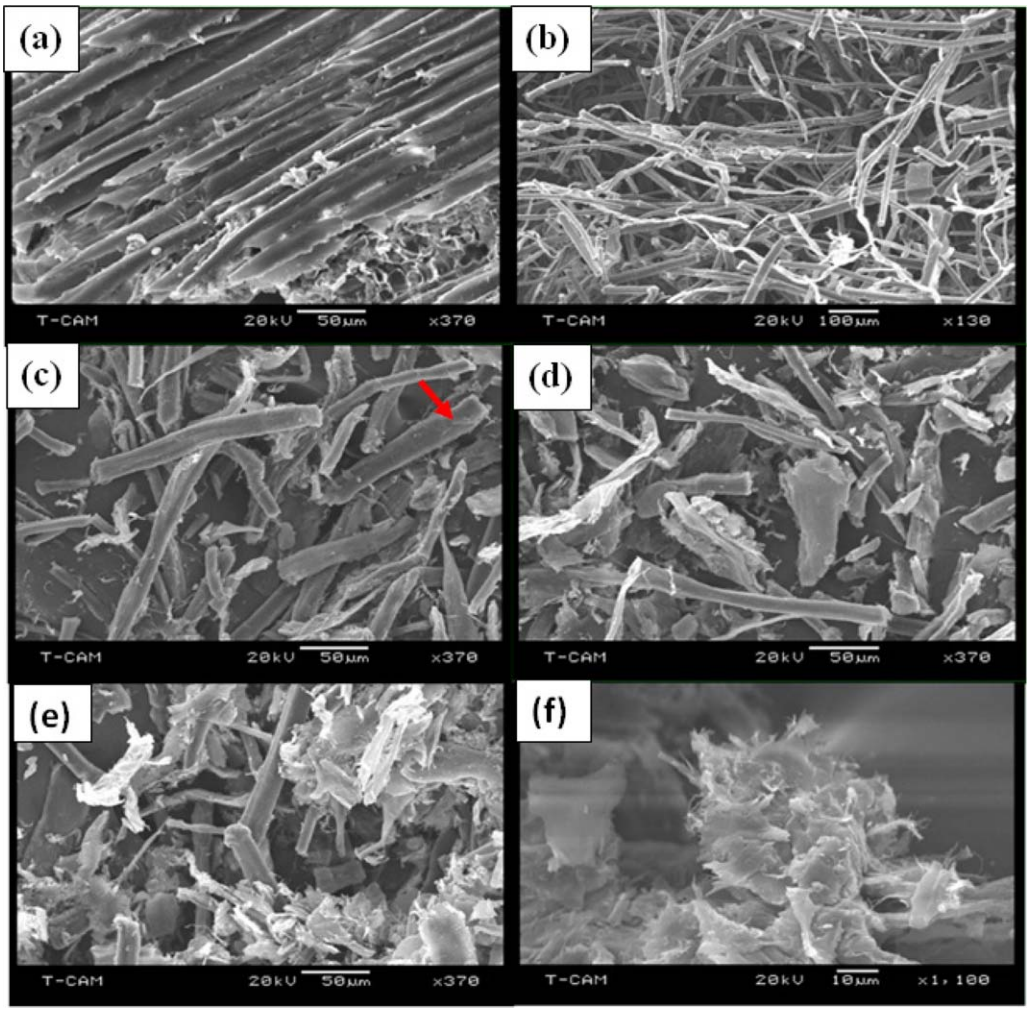

Figure 4. SEM micrograph of (a) wheat straw, (b) cellulose, (c) B-30 mins, (d) B-60 mins, (e) B-90 mins, and (f) B-120 mins (CNFs). [Color figure can be viewed in the online issue, which is available at wileyonlinelibrary.com.]

and kenaf fibers was in the order of several hundred micrometers. Unlike the synthetic fibers like carbon and glass, natural fibers are made of bundles containing fibrils that are in micron size, hence the word microfibrils. This is very commonly used while describing natural fibers.

Figures 3(b) and 4(b) show micrographs of bleached cellulose indicating individual fibers after the removal of hemicelluloses, lignin, and pectin around the fiber-bundles during chemical treatment. After chemical treatment, the amorphous materials (lignin, hemicellulose etc.) are removed from the inner part of the fiber via depolymerization and defibrillation. Thus, the diameter of the fibrils is reduced by a great extent.

SEM images of ball milled sample revealed an extraordinary effect of ball milling on the shape and size of the cellulose. Reduction of fiber length and diameter was observed after ball milling. Addition of ethanol/water mixture as solvent facilitated intra-fibril swelling. After 30 min of ball milling, the amorphous region of cellulose started to degrade thereby reducing fiber dimensions. This might be due to the fact that pure celluloses are made of crystalline and amorphous domain. Crystalline regions are resistant to mechanical stress developed in the ball mill during ball milling process, since in crystalline structure, cellulose molecules are subjected to extensive hydrogen bonding[36,40] and van der Waals forces.[35,36] On the other hand, amorphous celluloses are sensitive to mechanical stress. During ball milling, some of the crystalline regions are also degraded along with amorphous regions as shown in Figures 3(c) and 4(c). During ball milling, the celluloses are subjected to strong mechanical forces, which initiate the fibrillation of fiber bundles. The mechanism of fibrillation is breaking down hydrogen bond by shear forces, which combined with impact forces causes transverse cleavage of cellulose fibers (as indicated by arrow in Figures 3(c) and 4(c)) along the longitudinal axis of the cellulose, and effectively weakening the interfibrillar hydrogen bonds, and converting bleached celluloses to highly web like entangled cellulose nanofibers (CNFs).[31]

Each cellulose microfiber is composed of several nanofibers, which are joined together by hydrogen bonding. As the ball milling time increases, this hydrogen bonding is broken causing separation of cellulose nanofibers as shown in Figures 3(f) and 4(f). After 120 min of ball milling, all of cellulose is completely converted into cellulose nanofibers (CNFs). It is usually difficult

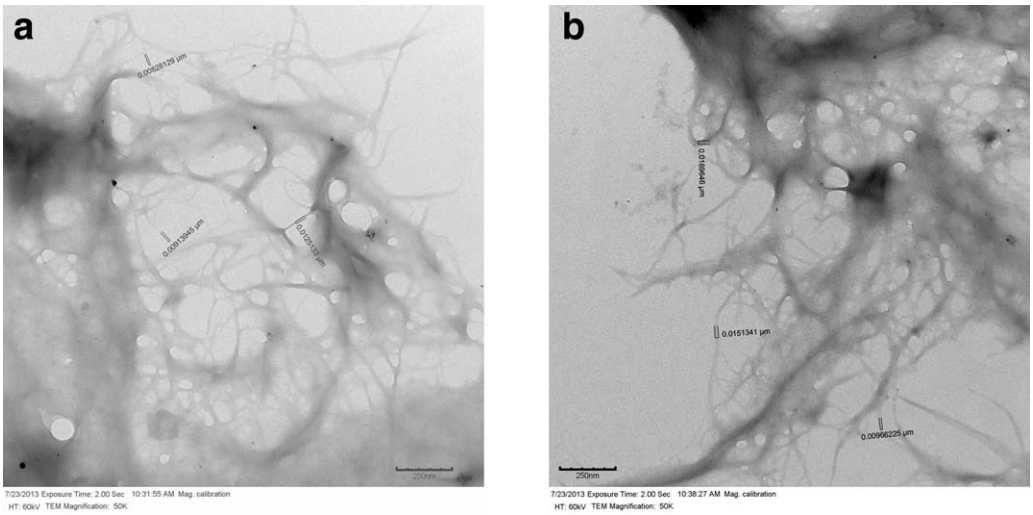

Figure 5. TEM images of CNFs from (a) kenaf fiber and (b) wheat straw.

to observe isolated individual nanofibers in SEM images since they are agglomerated together due to strong hydrogen bonding acting between them. TEM images revealing the web like cellulose nanofibers isolated after 120 min ball milling are shown in Figure 5. Exact length of CNFs was not measured in this study as ends of nanofibers could not be discerned and the fibrils were not straight.

The microscopic images of kenaf fibers and wheat straw are different. From Figures 4 and 5, it is obvious that the diameter of untreated kenaf fibers is around 100 μm while that of wheat straw is more than 500 μm. Diameter of bleached cellulose and cellulose nanofibers was also determined, and its size distribution graphs are presented in Figure 6. From distribution curve, it can be seen that most of the cellulose fibers are in the range of 14–16 μm (about 40–50% of total fibers). From distribution curves, it can be seen that ball milling treatment effectively isolates cellulose nanofibers from bleached celluloses. The diameter of most of the extracted cellulose nanofibers is approximately in the range of 21–30 nm, which account for 40–66% of total fibers.

FTIR Spectroscopy Analysis

Figures 7 and 8 show results of FTIR spectra obtained for kenaf fiber, wheat straw, bleached cellulose, cellulose after ball milling at different time intervals. Peaks observed at wavenumber 3275 cm^{-1} are indicative of O—H stretching band, which is due to the vibrations of the hydrogen bonded hydroxyl group.[2,16] The peaks at 2920 cm^{-1} and 2854 cm^{-1} were due to aliphatic saturated C—H stretching vibration. The presence of the peak at 1734 cm^{-1} in kenaf fiber and wheat straw is associated with the C=O stretching vibration of the acetyl and uronic ester groups. These groups are known to be present in pectin, hemicellulose, and/or an ester linkage of carboxylic group of ferulic and p-coumaric acids also known to be present in lignin and hemicellulose.[3,41,42] This peak was absent in the spectra obtained for bleached cellulose fibers (obtained from organosolv treatment and bleaching), ball milled cellulose, and cellulose nanofibers due to the removal of lignin and hemicellulose. The band at 1643 cm^{-1} was due to the bending mode of absorbed water since pure cellulose has a strong affinity for water.[43] The peak at 1514 cm^{-1} is associated with aromatic C=C stretching from aromatic ring of lignin.[41,44] No discernable change in this peak for ball milled samples may indicate that there could be still some traces of lignin present with celluloses. The smallest peak at 1465 cm^{-1} is due to the CH_2 symmetrical bending mode of the pyran ring. The weak peaks at 1427, 1365, and 1327 cm^{-1} represent C—H stretch and C—H or O—H bending[43] which can be seen in untreated and treated kenaf fibers and wheat straw. The peaks at 1030 and 914 cm^{-1} are indicative of C—O stretching and C—H deformation vibrations associated with cellulose,[1,18] and can be seen in all spectra. No distinguishable difference was observed in the spectra of cellulose nanofibers and cellulose fibers, suggesting that no changes in the molecular structure of cellulose occurred during ball milling.

In order to evaluate the relationship between morphology and cellulose structure, hydrogen bonds that exist in kenaf fiber, wheat straw, cellulose, acid hydrolyzed CNFs, and ball milled cellulose was analyzed by IR analysis. The broad band around 3200–3500 cm^{-1}, which is due to the O—H stretching vibration indicate inter-molecular hydrogen bond at O(6)H—O(2) and intra-molecular hydrogen bond at O(3)H—O(5).[33] All cellulose fibers show similar result but in case of B-120 mins (CNFs), these bands became lower in intensity and shift towards slightly higher wavelength. This is due to scission of the intra- and inter-molecular hydrogen bonds, thus indicating an increase in free hydroxyl groups.[45] This result can be further confirmed by the shift of the band from 2800–2900 cm^{-1} towards higher wavelength and decrease in intensity. All the results from FTIR analysis indicate that the isolated cellulose nanofibers retain their original molecular structure.

X-ray Diffraction Studies

Celluloses are crystalline in nature while lignin and hemicellulose are amorphous and therefore crystallinity of the fibers can be improved by the removal of these constituents. X-ray diffraction studies were conducted on wheat straw, kenaf fiber, bleached cellulose, and ball milled celluloses at different time

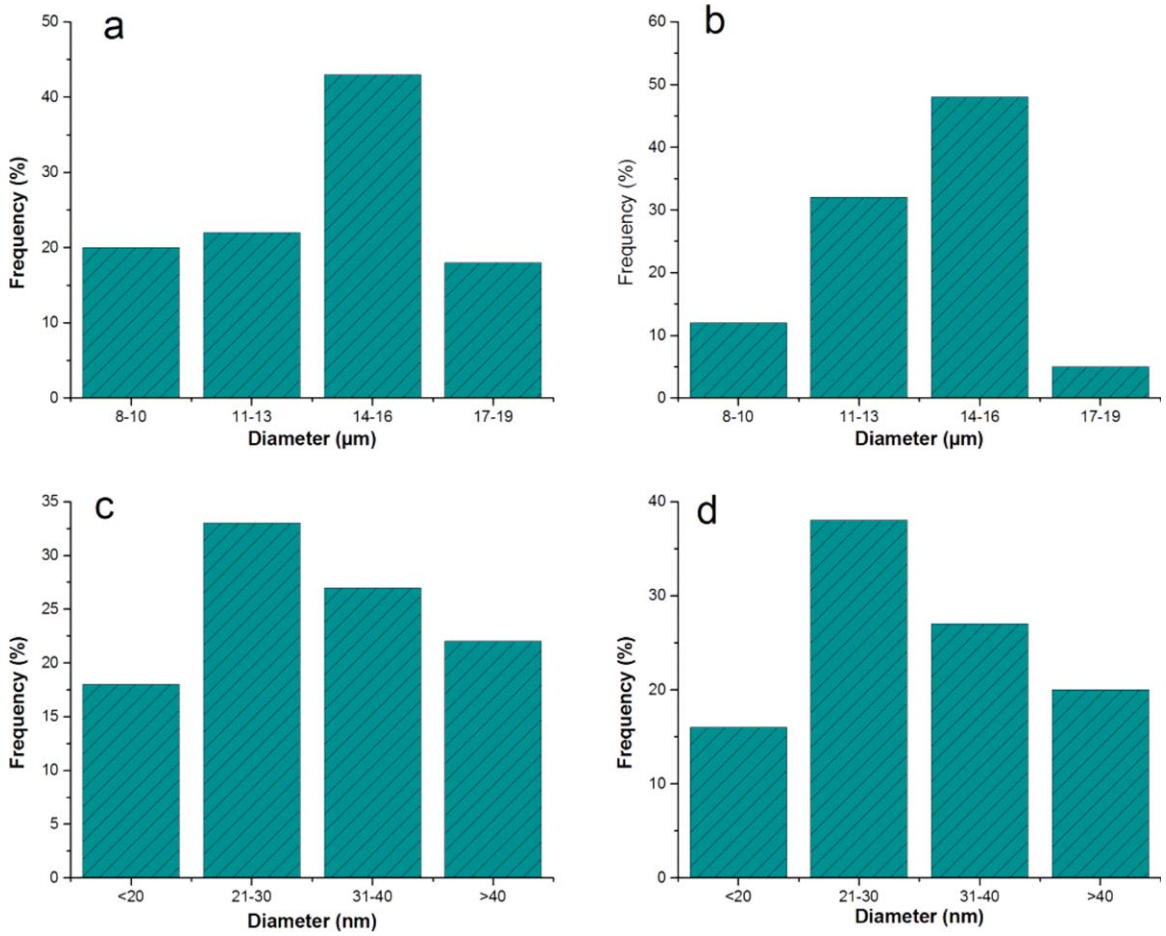

Figure 6. Size distribution curves of (a) K-Cellulose, (b) W-Cellulose, (c) CNFs from kenaf fiber, and (d) CNFs from wheat straw. [Color figure can be viewed in the online issue, which is available at wileyonlinelibrary.com.]

intervals to establish influence of chemical treatments and ball milling on crystallinity of the final fibers. Figures 9 and 10 show the XRD profile of treated and untreated kenaf fiber and wheat straw. Results of XRD studies show two weaker peaks around 2θ value of 14.8° and 16.4° and a sharp peak around 22.40°, which is the characteristic of typical forms of cellulose I.[46,47] The presence of these peaks in all samples indicates that crystal structure of cellulose was not changed during the chemical and

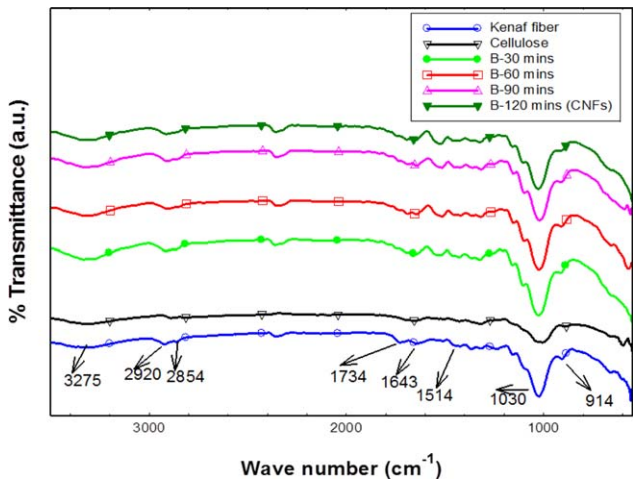

Figure 7. FTIR spectra of kenaf fiber, cellulose, and ball milled cellulose. [Color figure can be viewed in the online issue, which is available at wileyonlinelibrary.com.]

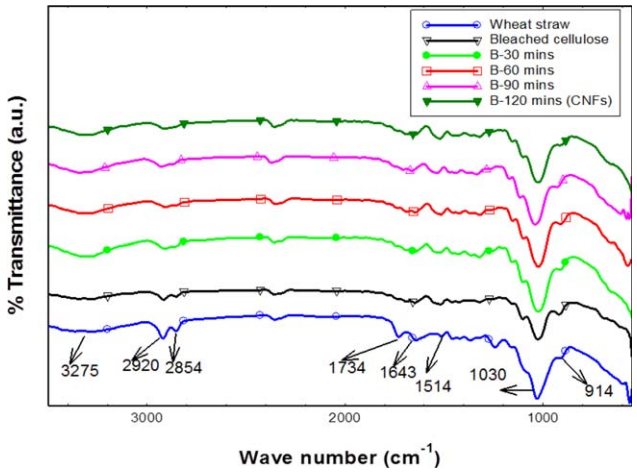

Figure 8. FTIR spectra of wheat straw, cellulose, and ball milled cellulose. [Color figure can be viewed in the online issue, which is available at wileyonlinelibrary.com.]

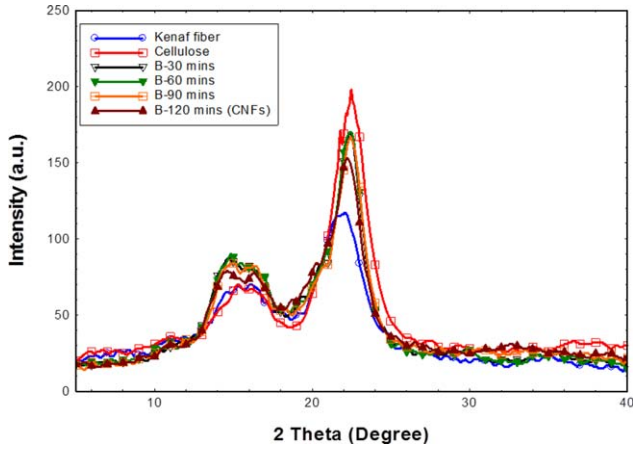

Figure 9. X-ray diffraction patterns of kenaf fiber; cellulose; and ball milled celluloses at different time interval. [Color figure can be viewed in the online issue, which is available at wileyonlinelibrary.com.]

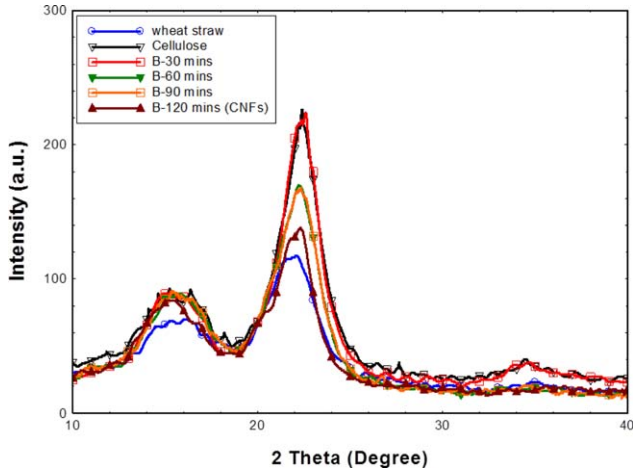

Figure 10. X-ray diffraction patterns of wheat straw; cellulose; and ball milled celluloses at different time interval. [Color figure can be viewed in the online issue, which is available at wileyonlinelibrary.com.]

ball milling treatments. This result is in contrast to those reported in some of the literatures[31,32,48] where the authors report that the celluloses converted into amorphous celluloses or cellulose II by ball milling technique. Ciolacu *et al.* reported that the ball milled cellulose regenerated in ethanol does show any peak corresponding to planes 101, 101, and 002.[45] Ago *et al.* studied the effect of ball milling on cellulose in presence of water solvent. He reported that cellulose I was transformed into cellulose II, indicated by the presence of peaks at 2θ value of 12.1°, 19.8°, and 22.0°.[32]

Table I. Crystallinity Index of Treated and Untreated Kenaf Fiber and Wheat Straw

Kenaf fiber	Crystallinity index (CI) %	Wheat straw	Crystallinity index (CI) %
Kenaf fiber	55.99 ± 1.0	Wheat straw	60.33 ± 0.71
Cellulose	77.88 ± 1.26	Cellulose	78.31 ± 0.69
B-30 mins	71.64 ± 0.64	B-30 mins	76.21 ± 0.15
B-60 mins	69.73 ± 0.45	B-60 mins	73.89 ± 0.33
B-90 mins	68.54 ± 0.40	B-90 mins	72.67 ± 1.39
B-120 mins (CNFs)	64.59 ± 0.16	B-120 mins (CNFs)	68.34 ± 0.34

The crystallinity index of each sample was calculated and results are presented in Table I. The crystallinity of untreated wheat straw (about 60% crystallinity) is higher than that of kenaf fibers (about 56% crystallinity). A significant increase in crystallinity was observed from untreated lignocellulosic biomass (55–60%) to bleached cellulose (77–78%). The increase in crystallinity was undoubtedly due to the removal of amorphous fractions such as hemicellulose and lignin. But crystallinity decreased by about 13–17% after ball milling for 120 min. This is due to the damage of the crystallites that occurred during high shearing action and friction force experienced by cellulose fibers during ball milling. The breakage of crystallites occurred through the breakdown of inter and intra hydrogen bonds which was confirmed from FTIR analysis as discussed earlier. Cellulose nanofibers obtained after ball milling at different time intervals maintained their crystallinity as cellulose I, even after slightly reduction of crystallinity and did not convert into cellulose II or amorphous celluloses.

From Tables I and II, it can be determined that the effect of ball milling on wheat straw is less than that of kenaf fibers (the crystallinity index of nanofibers obtained from wheat straw and kenaf are 68 and 64%, respectively). This might be due to the fact that cellulose obtained from kenaf fibers contains comparatively more amorphous phase (crystalline index is 77.88%) than

Table II. Summary of Thermogravimetric Analysis of Kenaf Fiber, Cellulose, and Ball Milled Cellulose

Sample	Weight loss due to moisture at 120°C (weight %)	Onset temperature (°C)	Maximum decomposition temperature (°C)
Kenaf fiber	8.0 ± 0.75	277.44 ± 2.75	316.01 ± 2.55
Cellulose	2.05 ± 0.35	330 ± 0.86	356.97 ± 0.94
B-30 mins	2.85 ± 0.28	322.93 ± 0.49	355.98 ± 0.46
B-60 mins	3.39 ± 0.08	316.99 ± 3.74	354.25 ± 1.04
B-90 mins	3.95 ± 0.73	312.40 ± 1.06	353.43 ± 1.01
B-120 mins (CNFs)	4.84 ± 0.29	308.27 ± 0.55	351.99 ± 0.47

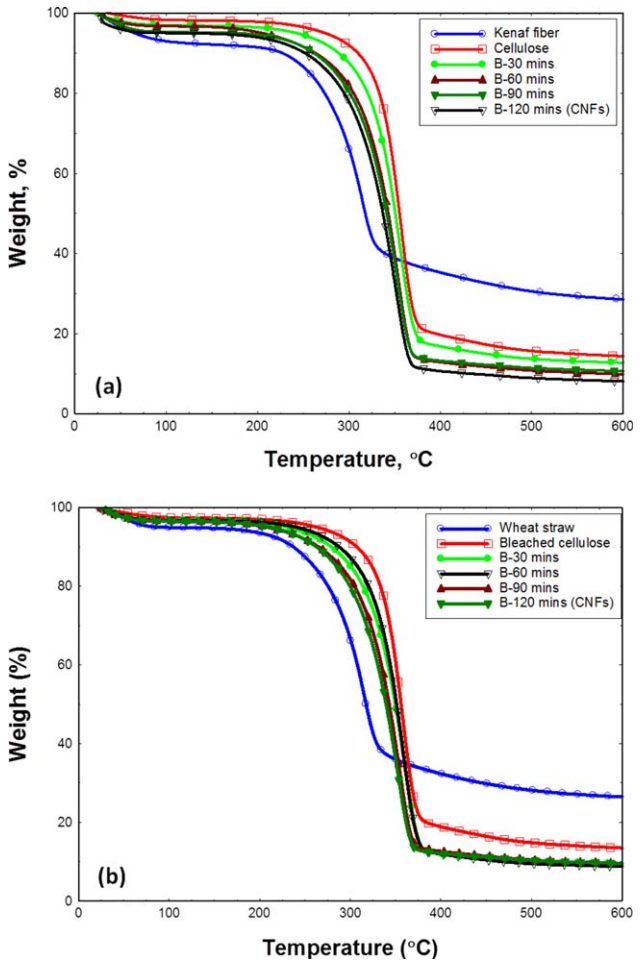

Figure 11. TG curve of (a) kenaf fiber, cellulose, and ball milled cellulose; and (b) wheat straw, cellulose, and ball milled cellulose. [Color figure can be viewed in the online issue, which is available at wileyonlinelibrary.com.]

that of cellulose obtained from wheat straw (crystalline index is 78.31%). During ball milling, these amorphous regions are more affected than crystalline regions as mentioned before.

Thermogravimetric Analysis (TGA)

TG graphs of wheat straw, kenaf fiber, bleached cellulose, ball milled celluloses at different time intervals are shown in Figure 11. From TGA graphs, it can be seen that the initial weight loss at around 120°C temperature was due to the evaporation of loosely bonded or H-bonded water molecules. Bleached cellulose contains relatively lower moisture content (2–2.6% by weight) than untreated fibers (moisture content was 5–8%) as shown in Tables II and III. This is due to the removal of hydrophilic constituents (hemicellulose and lignin) of raw fibers (wheat straw and kenaf fiber). Hemicellulose, lignin, and other non-cellulosic components of untreated fibers are hydrophilic in nature, which help to hold moisture in greater proportion.[16] The weight loss of kenaf fibers at 120°C is 8% while that of wheat straw is nearly 6%. Since kenaf fibers contain more amorphous constituents than wheat straw, it can entrap higher amount of water molecules.

However, the moisture content of cellulose increases upon ball milling. This might be due to the exposure of free hydroxyl groups. Ago *et al.* studied the effect of ball milling and they found that the breakage of inter and intramolecular hydrogen bonds in cellulose resulted in an increase in free hydroxyl groups.[33]

From Tables II and III, it can be seen that the degradation of untreated wheat straw and kenaf fibers started at around 276°C while for bleached cellulose, the onset of degradation began at about 330°C and degradation was maximum at about 357°C. Therefore, it is clear that FA/AA, PFA/PAA, and H_2O_2 treatment increases the degradation temperature, which was attributed to the removal of amorphous materials and the high degree of structural order of cellulose.[2] Thus, there is a relationship between structure and the thermal degradation of cellulose. It can be assumed that the existence of lignin, hemicellulose, and other non-cellulosic constituents lead to early onset of degradation of the wheat straw and kenaf fiber. Cellulose structure was dense and compact in bleached cellulose increases the onset temperature of decomposition. Due to ball milling of cellulose, the decomposition temperature of the cellulose slightly decreased. This might be due to the disturbance of some crystalline region during ball milling (as apparent from XRD analysis). From the decomposition temperature data (Tables II and III), it can be implied that thermal stability of the cellulose nanofibers did not change significantly due to ball milling treatment. This result is also in agreement with the results obtained from the XRD and FTIR analyses, indicating that the ball milling treatment for optimum time and in the presence of ethanol/water mixture did not change cellulose chemical composition and thermal stability.

Table III. Summary of Thermogravimetric Analysis of Wheat Straw, Cellulose, and Ball Milled Cellulose

Sample	Weight loss due to moisture at 120°C (weight %)	Onset temperature (°C)	Maximum decomposition temperature (°C)
Wheat straw	5.77 ± 0.86	276.79 ± 0.85	316.65 ± 0.71
Cellulose	2.59 ± 0.14	332.52 ± 0.70	359.28 ± 0.49
B-30 mins	3.09 ± 0.35	324.62 ± 0.77	358.97 ± 0.93
B-60 mins	3.13 ± 0.14	318.51 ± 0.78	357.94 ± 1.37
B-90 mins	3.69 ± 0.25	314.93 ± 1.75	354.86 ± 1.11
B-120 mins (CNFs)	4.14 ± 0.72	309.10 ± 1.61	353.04 ± 0.86

CONCLUSIONS

This research presents a detailed analysis of the effect of organic acids (Formic and acetic acid) and hydrogen peroxide on the removal of lignin and hemicellulose and also the effect of ball milling treatment on crystallinity and thermal properties of celluloses. Ball milling for 2 h successfully isolated cellulose nanofibers with maximum crystallinity and thermal stability. FTIR and XRD analyses showed that lignin and hemicellulose were significantly removed from kenaf fiber and wheat straw, and isolated cellulose nanofibers retained their original cellulose structure. Crystallinity of cellulose nanofibers from kenaf fibers was less than that of cellulose nanofibers from wheat straw. A homogeneous cellulose nanofiber of 8–100 nm in diameter was obtained from these processes. Thermal stability of kenaf, wheat straw, chemically treated fiber, and extracted CNFs were analyzed and the results showed that chemically treated celluloses possess much higher thermal stability than that of raw biomass but there is no significant change in thermal stability after ball milling. Ball milled nanofibers obtained from kenaf fibers and wheat straw show similar thermal stability.

ACKNOWLEDGMENTS

The authors are grateful to the NSF-CREST (Grant No. 1137681) and NSF-EPSCOR (Grant No. 1158862) for financial support to carry out this research.

REFERENCES

1. Alemdar, A.; Sain, M. *Bioresour. Technol.* **2008**, *99*, 1664.
2. Kaushik, A.; Singh, M. *Carbohydr. Res.* **2011**, *346*, 76.
3. Nuruddin, M.; Chowdhury, A.; Haque, S. A.; Rahman, M.; Farhad, S. F.; Jahan, M. S.; Quaiyyum, A. *Cellul. Chem. Technol.* **2011**, *45*, 347.
4. Wu, R.-L.; Wang, X.-L.; Li, F.; Li, H.-Z.; Wang, Y.-Z. *Bioresour. Technol.* **2009**, *100*, 2562.
5. Saha, B. C.; Nichols, N. N.; Cotta, M. A. *Bioresour. Technol.* **2011**, *102*, 10892.
6. Saha, B. C.; Iten, L. B.; Cotta, M. A.; Wu, Y. V. *Process Biochem.* **2005**, *40*, 3693.
7. Cetin, N. S.; Özmen, N. *Int. J. Adhes. Adhes.* **2002**, *22*, 477.
8. Tejado, A.; Pena, C.; Labidi, J.; Echeverria, J. *Bioresour. Technol.* **2007**, *98*, 1655.
9. Siqueira, G.; Bras, J.; Dufresne, A. *Polymers* **2010**, *2* 728.
10. Das, K.; Ray, D.; Bandyopadhyay, N. R.; Sahoo, S.; Mohanty, A. K.; Misra, M. *Compos. B Eng.* **2011**, *42*, 376.
11. Fleming, K.; Gray, D. G.; Matthews, S. *Chem. Eur. J.* **2001**, *7*, 1831.
12. Dahlke, B.; Larbig, H.; Scherzer, H.; Poltrock, R. *J. Cell. Plast.* **1998**, *34*, 361.
13. Azizi Samir, M. A. S.; Alloin, F.; Dufresne, A. *Biomacromolecules* **2005**, *6*, 612.
14. Orts, W. J.; Shey, J.; Imam, S. H.; Glenn, G. M.; Guttman, M. E.; Revol, J.-F. *J. Polym. Environ.* **2005**, *13*, 301.
15. Nishino, T.; Matsuda, I.; Hirao, K. *Macromolecules* **2004**, *37*, 7683.
16. Mandal, A.; Chakrabarty, D. *Carbohydr. Polym.* **2011**, *86*, 1291.
17. Dong, X. M.; Revol, J.-F.; Gray, D. G. *Cellulose* **1998**, *5*, 19.
18. Li, R.; Fei, J.; Cai, Y.; Li, Y. *Carbohydr. Polym.* **2009**, *76*, 94.
19. Herrick, F. W.; Casebier, R. L.; Hamilton, J. K.; Sandberg, K. R. *J. Appl. Polym. Sci. Appl. Polym. Symp.* **1983**, *37*, 797.
20. Turbak, A. F.; Snyder, F. W.; Sandberg, K. R. *J. Appl. Polym. Sci. Appl. Polym. Symp.* **1983**, *37*, 815.
21. Hayashi, N.; Kondo, T.; Ishihara, M. *Carbohydr. Polym.* **2005**, *61*, 191.
22. Henriksson, M.; Henriksson, G.; Berglund, L.; Lindström, T. *Eur. Polym. J.* **2007**, *43*, 3434.
23. Saito, T.; Nishiyama, Y.; Putaux, J. L.; Vignon, M.; Isogai, A. *Biomacromolecules* **2006**, *7*, 1687.
24. Saito, T.; Kimura, S.; Nishiyama, Y.; Isogai, A. *Biomacromolecules* **2007**, *8*, 2485.
25. Chen, W.; Yu, H.; Liu, Y.; Chen, P.; Zhang, M.; Hai, Y. *Carbohydr. Polym.* **2011**, *83*, 1804.
26. Chen, W.; Yu, H.; Liu, Y.; Hai, Y.; Zhang, M.; Chen, P. *Cellulose* **2011**, *18*, 433.
27. Cheng, Q.; Wang, S.; Rials, T. G. *Compos. Appl. Sci. Manuf.* **2009**, *40*, 218.
28. Louidi, S.; Bentayeb, F.-Z.; Suñol, J.; Escoda, L. *J. Alloys Comp.* **2010**, *493*, 110.
29. Liu, T. Yi.; Ma, Y.; Yu, S. F.; Shi, J.; Xue, S. *Innovat. Food Sci. Emerg. Technol.* **2011**, *12*, 586.
30. Maier, G.; Zipper, P.; Stubicar, M.; Schurz, J. *Cellul. Chem. Technol.* **2005**, *39*, 167.
31. Avolio, R.; Bonadies, I.; Capitani, D.; Errico, M. *Carbohydr. Polym.* **2012**, *87*, 265.
32. Ago, M.; Endo, T.; Hirotsu, T. *Cellulose* **2004**, *11*, 163.
33. Ago, M.; Endo, T.; Okajima, K. *Polym. J.* **2007**, *39*, 435.
34. Nishiyama, Y.; Langan, P.; Chanzy, H. *J. Am. Chem. Soc.* **2002**, *124*, 9074.
35. Notley, S. M.; Pettersson, B.; Wågberg, L. *J. Am. Chem. Soc.* **2004**, *126*, 13930.
36. Yamashita, Y.; Sasaki, C.; Nakamura, Y. *Carbohydr. Polym.* **2010**, *79*, 250.
37. Inoue, H.; Yano, S.; Endo, T.; Sakaki, T.; Sawayama, S. *Biotechnol. Biofuels* **2008**, *1*, 1.
38. Watkins, D.; Nuruddin, M.; Hosur, M.; Jeelani, S. *J. Mater. Res. Technol.* **2015**, *4*, 26.
39. Penjumras, P.; Abdul Rahman, R.; Talib, R. A.; Abdan, K. *The Scientific World Journal* **2015**, 293609. Available at: http://doi.org/10.1155/2015/293609.
40. Nishiyama, Y.; Sugiyama, J.; Chanzy, H.; Langan, P. *J. Am. Chem. Soc.* **2003**, *125*, 14300.
41. Sain, M.; Panthapulakkal, S. *Ind. Crops Prod.* **2006**, *23*, 1.

42. Sun, X. F.; Xu, F.; Sun, R. C.; Fowler, P.; Baird, M. S. *Carbohydr. Res.* **2005**, *340*, 97.

43. Jiang, M.; Zhao, M.; Zhou, Z.; Huang, T. *Ind. Crops Prod.* **2011**, *33*, 734.

44. Sun, R.; Tomkinson, J.; Wang, Y.; Xiao, B. *Polymer* **2000**, *41*, 2647.

45. Ciolacu, D.; Ciolacu, F.; Popa, V. I. *Cellul. Chem. Technol.* **2011**, *45*, 13.

46. Tonoli, G. H. D.; Teixeira, E. M.; Corrêa, A. C.; Marconcini, J. M.; Caixeta, L. A.; Pereira-da-Silva, M. A.; Mattoso, L. H. C. *Carbohydr. Polym.* **2012**, *89*, 80.

47. Nuruddin, M.; Tcherbi-Narteh, A.; Hosur, M.; Jeelani, S. CAMX Conference, Orlando, FL, **2014**.

48. Paes, S. S.; Sun, S.; MacNaughtan, W.; Ibbett, R.; Ganster, J.; Foster, T. J.; Mitchell, J. R. *Cellulose* **2010**, *17*, 693.